

The Apoplastic Oxidative Burst Peroxidase in *Arabidopsis* Is a Major Component of Pattern-Triggered Immunity

Arsalan Daudi,^{a,1} Zhenyu Cheng,^{b,c} Jose A. O'Brien,^{a,2} Nicole Mammarella,^{b,c} Safina Khan,^a Frederick M. Ausubel,^{b,c} and G. Paul Bolwell^{a,3}

^aSchool of Biological Sciences, Royal Holloway, University of London, Egham, Surrey TW20 0EX, United Kingdom

^bDepartment of Genetics, Harvard Medical School, Boston, Massachusetts 02115

^cDepartment of Molecular Biology, Massachusetts General Hospital, Boston, Massachusetts 02114

In plants, reactive oxygen species (ROS) associated with the response to pathogen attack are generated by NADPH oxidases or apoplastic peroxidases. Antisense expression of a heterologous French bean (*Phaseolus vulgaris*) peroxidase (FBP1) cDNA in *Arabidopsis thaliana* was previously shown to diminish the expression of two *Arabidopsis* peroxidases (peroxidase 33 [PRX33] and PRX34), block the oxidative burst in response to a fungal elicitor, and cause enhanced susceptibility to a broad range of fungal and bacterial pathogens. Here we show that mature leaves of T-DNA insertion lines with diminished expression of PRX33 and PRX34 exhibit reduced ROS and callose deposition in response to microbe-associated molecular patterns (MAMPs), including the synthetic peptides Flg22 and Elf26 corresponding to bacterial flagellin and elongation factor Tu, respectively. PRX33 and PRX34 knockdown lines also exhibited diminished activation of Flg22-activated genes after Flg22 treatment. These MAMP-activated genes were also downregulated in unchallenged leaves of the peroxidase knockdown lines, suggesting that a low level of apoplastic ROS production may be required to preprime basal resistance. Finally, the PRX33 knockdown line is more susceptible to *Pseudomonas syringae* than wild-type plants. In aggregate, these data demonstrate that the peroxidase-dependent oxidative burst plays an important role in *Arabidopsis* basal resistance mediated by the recognition of MAMPs.

INTRODUCTION

Plants have evolved sophisticated surveillance systems triggered by recognition of microbe-associated molecular patterns (MAMPs), molecules such as eubacterial flagellin or peptidoglycan (PGN) or fungal chitin, which plants use to identify the presence of potentially harmful microbes. The plant defense response has now been dissected into several tiers of preexisting and/or activated defenses, many of which seem to involve the production of reactive oxygen species (ROS) (Chisholm et al., 2006; Jones and Dangl, 2006; He et al., 2007). The primary ROS studied to date include superoxide, hydrogen peroxide, and nitric oxide, which function either directly in the establishment of defense mechanisms or indirectly via synergistic interactions with other signaling molecules, such as salicylic acid (reviewed in Bolwell and Daudi, 2009). The major sources of ROS during most biotic stress responses seem to be plasma membrane-localized

NADPH/NADH oxidases that generate superoxide, or cell wall-localized peroxidases that generate hydrogen peroxide, or both systems operating in tandem (Bolwell, 1999). To elucidate the underlying biochemical and physiological mechanisms involved in the plant defense response to pathogen attack, it is important to dissect the relative contributions of NADPH oxidases and peroxidases in the production of ROS in both basal resistance and in the so-called hypersensitive response (HR) (Bolwell et al., 1998; Martinez et al., 1998; Bolwell, 1999; J.J. Grant et al., 2000; M. Grant et al., 2000; Torres et al., 2002; Bolwell and Daudi, 2009). By definition, basal resistance or pattern-triggered immunity (PTI) refers to defense responses activated by the perception of MAMPs. The class of responses encompassing gene-for-gene resistance and the hypersensitive response, now collectively termed effector-triggered immunity (ETI), includes defenses activated by recognition of microbial virulence factors (effectors) that target PTI or other key host functions.

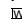
Well-studied MAMP elicitors of ROS production or the oxidative burst include the synthetic peptides Flg22 and Elf26, which correspond to conserved epitopes of bacterial flagellin and elongation factor Tu (EF-Tu), respectively. Hydrolytic enzymes, including chitinases, xylanases, or polygalacturonases, may also elicit ROS by generating chitin oligomers, β -1,3-glucans, or oligogalacturonides (OGs), respectively. Partially purified extracellular matrix preparations derived from fungal pathogens, such as *Fusarium oxysporum*, can also be used to elicit PTI. After interaction of MAMPs with the relevant host plant receptor, a series of well-defined and conserved events occurs in all plant species examined, among which an increase in cytosolic Ca^{2+} ,

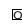
¹Current address: Department of Plant Pathology, University of California, Davis, CA, 95616.

²Current address: Department of Plant Systems Biology, Vlaams Instituut voor Biotechnologie, B-9052 Ghent, Belgium; Department of Plant Biotechnology and Genetics, Ghent University, B-9052 Ghent, Belgium.

³Address correspondence to p.bolwell@rhul.ac.uk.

The author responsible for distribution of materials integral to the findings presented in this article in accordance with the policy described in the Instructions for Authors (www.plantcell.org) is: Frederick M. Ausubel (ausubel@molbio.mgh.harvard.edu).

 Online version contains Web-only data.

 Open Access articles can be viewed online without a subscription. www.plantcell.org/cgi/doi/10.1105/tpc.111.093039

often measured within seconds of elicitation, is believed to be a primary signal essential for several downstream events (Chandra et al., 1997; M. Grant et al., 2000). In addition to this early calcium influx, a rapid efflux of K^+ and Cl^- and extracellular alkalinization of cell cultures has been measured in response to MAMP elicitation (Fellbrich et al., 2000).

NADPH oxidases, also referred to as respiratory burst oxidases, have been implicated in biotic interactions, abiotic stress responses, and development in different plant species and have been studied in detail in *Arabidopsis thaliana* (Torres and Dangl, 2005). Among the members of the 10-gene family of *RBOH* genes encoding homologs of the mammalian NADPH oxidase gp91^{phox} (Keller et al., 1998; Torres et al., 1998), *RBOHD* and *RBOHF* were found to be required for the production of a full oxidative burst in response to avirulent strains of the bacterial and oomycete pathogens *Pseudomonas syringae* and *Hyaloperonospora arabidopsidis*, respectively (Torres et al., 2002).

Although *RBOHD* and *RBOHF* seem to play crucial roles in *Arabidopsis* in the generation of ROS in response to pathogen attack, *rbohD* mutants do not appear to be more susceptible to a virulent strain of *P. syringae*, whereas *rbohF* mutants exhibit a modest level of enhanced susceptibility (Chaouch et al., 2011). Torres et al. (2005) suggest that instead of generating ROS that act directly as antimicrobial agents or in the activation of defense response pathways, the major role of NADPH oxidases may be to limit the spread of salicylic acid–mediated cell death in cells surrounding an infection site (Torres et al., 2005). This conclusion was based on the observation that a *lesion stimulating disease 1 (lsd1)-rbohD-rbohF* triple mutant exhibits spreading lesions. In the absence of the *rbohD* and *rbohF* mutations, *lsd1* mutants form spontaneous lesions in the absence of pathogen attack, but these lesions remain localized. Torres et al. (2005) also showed that NADPH oxidases need to be activated by an independent source of ROS to generate their own oxidative burst. It is thus possible that the ROS that activates *RBOHD* and *RBOHF* is generated by peroxidases during the basal (PTI) defense response, in which case NADPH oxidases may function mainly in the HR. On the other hand, a relatively limited role for NADPH oxidases in the HR has been observed in tobacco (*Nicotiana tabacum*), where *rbohD*-mediated hydrogen peroxide production does not seem to be essential for the development of the HR or systemic acquired resistance (SAR) (Rouet et al., 2006; Lherminier et al., 2009). SAR is a whole plant resistance response that is normally triggered by an HR and spreads systemically from a localized site of infection to distal parts of the plant, mediated by salicylic acid.

The apoplastic peroxidase-dependent oxidative burst was first proposed by Bach and coworkers (Bach et al., 1993), who showed that the cell wall is required for a full oxidative burst in carrot (*Daucus carota*) cultured cells. This mechanism has now been validated in French bean (*Phaseolus vulgaris*) (Bolwell et al., 1998; Bolwell, 1999), *Arabidopsis* (Bindschedler et al., 2006; Davies et al., 2006), *Capsicum annuum* (Choi et al., 2007), *Lactuca sativa* (Bestwick et al., 1998), and *Gossypium hirsutum* (Martinez et al., 1998). Although pharmacological inhibitor-based studies have implicated peroxidases as key components in ROS production in the defense response (J.J. Grant et al., 2000; Soyulu et al., 2005), there has been relatively little investigation of

peroxidase-dependent ROS production in *Arabidopsis*. We previously identified an *Arabidopsis* sodium azide-sensitive but diphenylene iodonium-insensitive apoplastic oxidative burst that generates H_2O_2 in response to a *Fusarium oxysporum* cell wall preparation (Bindschedler et al., 2006; Davies et al., 2006). Inhibition of an oxidative burst by diphenylene iodonium with an I_{50} of $\sim 0.2 \mu M$ is indicative of the involvement of an NADPH/NADH oxidase, whereas inhibition by sodium azide with an I_{50} greater than $50 \mu M$ suggests a peroxidase-dependent mechanism (Bolwell et al., 1998; Frahy and Schopfer, 1998).

Because the *Arabidopsis* genome encodes at least 73 class III peroxidases (Welinder et al., 2002; Oliva et al., 2009), which complicates genetic analysis, we constructed transgenic *Arabidopsis* plants expressing an antisense cDNA encoding a French bean class III peroxidase (*FBP1*) with the goal of knocking down expression of key *Arabidopsis* peroxidases involved in ROS generation during the defense response (Bindschedler et al., 2006). Importantly, transgenic *FBP1* plants exhibited an impaired oxidative burst and were more susceptible than wild-type plants to both fungal and bacterial pathogens. Genome-wide transcriptional profiling and RT-PCR analysis showed that the antisense *FBP1* transgenic *Arabidopsis* plants had reduced levels of two class III peroxidase mRNAs corresponding to the *Arabidopsis* genes *At 3g49120 (PCb; PRX34)* and *At 3g49110 (PCa; PRX33)*. These data suggested that peroxidases play a significant role in generating H_2O_2 during the *Arabidopsis* defense response and in conferring resistance to a wide range of pathogens.

Because our previous work with the *Arabidopsis* antisense *FBP1* transgenic plants showed that functional peroxidases were required for the production of ROS in response to a fungal cell wall elicitor, we hypothesized that peroxidases may catalyze ROS production during basal resistance triggered by recognition of MAMPs and that this initial oxidative burst may be essential for the activation of basal defenses associated with PTI. This might explain why the *FBP1* antisense lines exhibited susceptibility to a broad range of pathogens. In this article, we further examine the role of apoplastic peroxidases in *Arabidopsis* PTI. We find that several independent lines with reduced expression of two key peroxidase genes, *PRX33* or *PRX34*, exhibit many defects in PTI in mature plants. An *rbohD* mutant is also impaired in some PTI-related responses, but to a lesser degree than the peroxidase knockdown lines.

RESULTS

Generation of Transgenic *Arabidopsis* Plants Expressing Antisense *FBP1* cDNA

We previously described the generation of a transgenic *Arabidopsis* line expressing a heterologous *FBP1* cDNA in an antisense orientation (Bindschedler et al., 2006). In these previous experiments, it was very challenging to maintain the transgenic antisense *FBP1* plants, because they succumbed to opportunistic infections. We were only able to recover a single viable line “*asFBP1.1 H₄*”, which we refer to in this article as *asFBP1.1*. The transgenic line *asFBP1.1* exhibited a reduced oxidative burst in response to a *Fusarium* cell wall elicitor preparation, reduced

expression of two cell wall peroxidase-encoding genes (*PRX33*; *At 3g49110* and *PRX34*; *At 3g49120*), and enhanced susceptibility to infection by bacterial and fungal pathogens (Bindschedler et al., 2006). Besides its hypersusceptibility to infection, *asFBP1.1* does not exhibit any obvious adverse phenotypes. Interestingly, however, the leaves of *asFBP1.1* at all stages of development after the formation of the rosette are ~50% larger than ecotype Columbia (Col-0) wild-type leaves, and *asFBP1.1* transgenic plants exhibit a delayed senescence phenotype of 7 to 10 d.

To overcome the difficulties of generating transgenic plants that constitutively express *FBP1* antisense cDNA, we also constructed transgenic Col-0 *Arabidopsis* plants in which the antisense *FBP1* cDNA was expressed under the control of a dexamethasone (dex)-inducible promoter (see Methods). In contrast with *asFBP1.1*, the dex-inducible lines did not exhibit any discernable developmental differences compared with wild-type Col-0 plants, including leaf size and time to senescence. Although it proved difficult to work with these dex-inducible lines, because there was a significant amount of variation from one experiment to another in the levels of *PRX33* and *PRX34* mRNAs after dex treatment, in several independent dex-inducible lines, dex-treated *FBP1* plants exhibited reduced levels of *PRX33* and/or *PRX34* mRNA compared with Col-0 plants (see Supplemental Figure 1A online) and enhanced susceptibility to *P. syringae* pv tomato strain DC3000 (see Supplemental Figure 1B online).

As described in Methods, PCR analysis of *asFBP1.1* revealed that the *FBP1* antisense cDNA construct is inserted into the second intron of gene *At 5g01075* (on chromosome 5), which is annotated on The Arabidopsis Information Resource (www.Arabidopsis.org) as encoding a β -galactosidase. No evidence was found in the literature to suggest that *At 5g01075* plays a role in pathogen defense signaling or basal resistance. Moreover, Genevestigator analysis (Hruz et al., 2008) revealed that *At5g01075* did not show any significant differential expression in response to treatment by several common biotic stresses or MAMPs (see Supplemental Figure 2 online). Finally, SALK line_084805C, which contains a homozygous T-DNA insertion in *At 5g01075* (the insertion site of the *FBP1* cDNA in *asFBP1.1*), exhibited a wild-type phenotype with respect to ROS accumulation after treatment with the *Fusarium* cell wall preparation and did not exhibit enhanced susceptibility to *P. syringae* pv tomato strain DC3000. Thus, these data indicate that the enhanced disease susceptibility phenotype of *asFBP1.1* is most likely not a consequence of the disruption of the gene into which the *asFBP1* transgene is inserted or to other off-target effects.

Some T-DNA Insertion Lines That Affect the Expression of *PRX33* and *PRX34* Mimic the Phenotype of *asFBP1.1*

To confirm the conclusion that the immunocompromised phenotype of *asFBP1.1* and the dex-inducible *FBP1* antisense lines is a consequence of diminished expression of *PRX33* and/or *PRX34*, we tested three T-DNA insertion lines (see Methods) in which the expression of *PRX33* and/or *PRX34* is affected. *PRX33* and *PRX34*, which are contiguous genes, show nearly 95% homology at the protein level, but their promoter and intronic sequences are highly divergent (Valério et al., 2004). Quantitative RT-PCR (qRT-PCR) analysis showed that the basal level of

PRX34 mRNA is 128-fold higher than the basal level of *PRX33* mRNA in wild-type Col-0 plants. The *prx33:T-DNA* knockdown line (ecotype Wassilewskija [WS]) contains an insertion in intron 1 of *At 3g49110* 660 bp downstream of the ATG initiation codon and could potentially be a hypomorphic mutant. The *prx34:T-DNA* knockdown line (ecotype Col-0) contains an insertion in the promoter region of *At 3g49120* 200 bp upstream of the ATG initiation codon and is most likely a hypomorphic mutation. The *prx33:T-DNA;prx34:RNAi* double knockdown line was obtained by transforming the *prx33:T-DNA* line with a *prx34:RNAi* construct (Passardi et al., 2006). Similarly to *asFBP1.1*, the *prx33:T-DNA*, *prx34:T-DNA*, and *prx33:T-DNA;prx34:RNAi* lines have larger leaves than Col-0 or WS (but smaller than *asFBP1.1*) and exhibit delayed senescence.

Figure 1A shows that the *prx34:T-DNA* line expresses low basal levels of *PRX34* mRNA but that *PRX33* expression is not affected. However, the T-DNA insertion in *PRX33* affects both *PRX33* and *PRX34* expression (Figure 1A). The double knockdown line, *prx33:T-DNA;prx34:RNAi*, expresses low levels of both *PRX33* and *PRX34* mRNAs. All three of these *PRX33* and/or *PRX34* knockdown lines exhibited highly diminished 3,3'-diaminobenzidine (DAB) staining after elicitation with a *Fusarium oxysporum* cell wall elicitor preparation (FoCWE) (Figures 2A and 2B; see Supplemental Figures 3 and 4 online). An image analysis-based scoring system using CellProfiler software (Carpenter et al. 2006) was devised to quantify the DAB staining data as shown in Figure 2. DAB staining is caused by an H₂O₂-dependent polymerization reaction that is catalyzed by peroxidases (Thordal-Christensen et al., 1997). However, it is unlikely that the diminished levels of DAB staining in the *PRX33* and *PRX34* knockdown lines are solely a consequence of diminished levels of total peroxidase activity rather than diminished ROS levels. The *Arabidopsis* genome encodes at least 73 class III peroxidases (Welinder et al., 2002; Oliva et al., 2009), and we showed previously in the *asFBP1.1* line that soluble peroxidase activity is not diminished and that bound peroxidase activity is only diminished ~50% (Bindschedler et al., 2006). Moreover, we also showed that ROS production in *asFBP1.1* is diminished using a xylenol orange assay (Bindschedler et al., 2006). Similarly, we have found a reduction in ROS production using a xylenol orange assay in transgenic tissue culture lines knocked down for *PRX33* and *PRX34* expression (J.A. O'Brien, unpublished data).

Similarly to *asFBP1.1*, the *prx33:T-DNA* and the *prx33:T-DNA;prx34:RNAi* lines were significantly more susceptible to *P. syringae* pv tomato strain DC3000 than the parent wild-type WS ecotype (Figure 3B). By contrast, *prx34:T-DNA* plants were not significantly more susceptible to *P. syringae* pv tomato strain DC3000 than Col-0 plants (Figure 3A), although in some experiments, they did exhibit a modest level of enhanced susceptibility.

Peroxidase Knockdown Lines Are Compromised in MAMP-Elicited Immune Responses

The observation that the oxidative burst elicited by the FoCWE is greatly diminished in the *asFBP1.1*, *prx33:T-DNA*, *prx34:T-DNA*, and *prx33:T-DNA;prx34:RNAi* lines (referred to collectively from now on as the *PRX33* and *PRX34* knockdown lines) (Figures 2A and 2B; see Supplemental Figures 3 and 4 online) suggested that

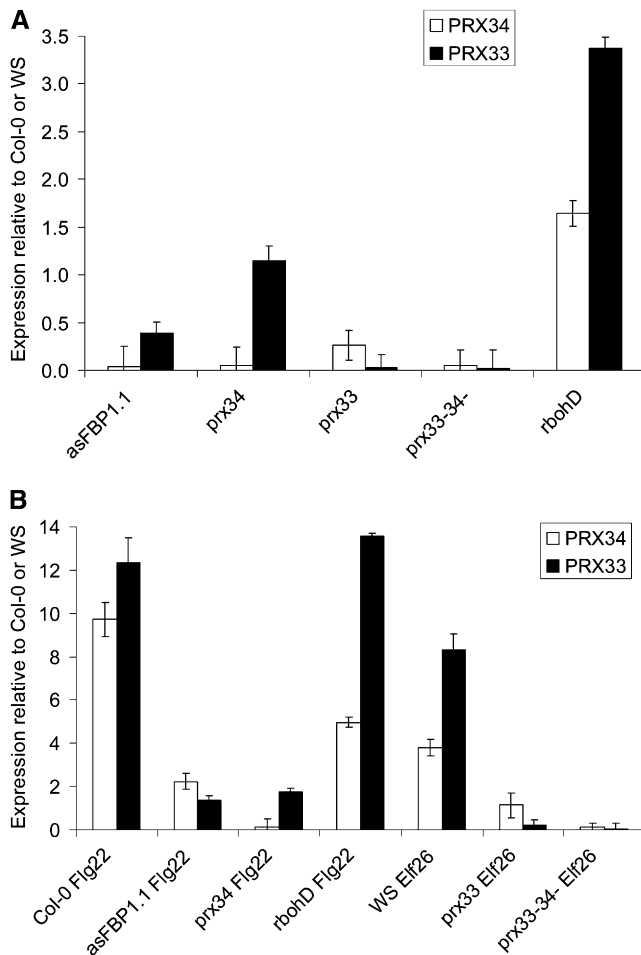


Figure 1. Downregulation of *PRX33* and *PRX34* Transcripts in Peroxidase T-DNA and Antisense Knockdown Lines.

(A) Quantitative RT-PCR analysis of *PRX33* and *PRX34* transcripts in 23- to 25-d old rosette leaves.

(B) Quantitative RT-PCR analysis of *PRX33* and *PRX34* transcripts in 4-week-old rosette leaves 2 h after infiltration of 0.5 μ M Flg22 or Elf26. Data represent the average \pm SD. All quantitative gene expression measurements were performed using technical and biological triplicates. The experiments were repeated at least two times with similar results. Values for the peroxidase T-DNA and antisense knockdown lines were found to be significantly different from *rbohD* with a P value < 0.05 as determined by Student's *t* test **(A)**. Values for the peroxidase T-DNA and antisense knockdown lines treated with Flg22 were found to be significantly different from Col-0, WS, and *rbohD* with a P value < 0.05 as determined by Student's *t* test **(B)**. *prx34*, *prx34:T-DNA*; *prx33*, *prx33:T-DNA*; *prx33-34-*, *prx33:T-DNA*; *prx34:RNAi*.

PRX33 and *PRX34* are involved in MAMP-mediated responses. This is based on the reasoning that the *FoCWE* contains many MAMPs that elicit an immune response. Indeed, all of the *PRX33* and *PRX34* knockdown lines exhibited significantly diminished DAB staining in response to diverse MAMPs, including the synthetic peptides Flg22 and Elf26 (Figures 2A and 2B; see Supplemental Figures 3 and 4 online) (which correspond to the

active epitopes of bacterial flagellin and EF-Tu, respectively), as well as PGN and an OG preparation derived from pectin (Figure 2C; see Supplemental Figure 5 online). As expected, *Arabidopsis* ecotype WS, which is a natural *fls2* mutant and the parent strain for the *prx33:T-DNA* insertion and the double knockdown *prx33:T-DNA*; *prx34:RNAi* lines, did not respond to Flg22 (Figure 2B; see Supplemental Figure 4 online). The WS ecotype, however, did respond to the other three well-characterized MAMPs (Elf26, PGN, and OG) that were tested as well as to *FoCWE*.

Col-0 wild-type leaves exhibited robust but different patterns of H_2O_2 accumulation in response to treatment with the different elicitors tested (Figures 2A and 2C; see Supplemental Figures 3 and 5 online). High levels of evenly distributed H_2O_2 accumulation were observed in Col-0 leaves treated with Flg22 and *FoCWE*, and slightly lower levels were observed after treatment with Elf26. Treatment with PGN and OG resulted in somewhat uneven and patchy H_2O_2 accumulation. By contrast, *asFBP1.1*, as well as the *prx34:T-DNA* lines (Col-0 background) showed very little if any ROS production in response to all of the elicitors tested (Figures 2A and 2C; see Supplemental Figures 3 and 5 online). In the case of ecotype WS plants, mature rosette leaves showed high and evenly distributed levels of ROS when challenged with Elf26, similarly to Col-0, but not with Flg22 for the reason stated above (Figure 2B; see Supplemental Figure 4 online). Compared with the wild-type WS plants, the *prx33:T-DNA* and *prx33:T-DNA*; *prx34:RNAi* lines generated in the WS genetic background showed a clear reduction in ROS accumulation after treatment with Elf26, PGN, OG, and *FoCWE* (Figures 2A and 2B; see Supplemental Figures 4 and 5 online). These results show that the *PRX33* and *PRX34* peroxidases play a major role in the generation of ROS in response to many different MAMP elicitors.

In addition to the activation of an oxidative burst, another well-studied MAMP-elicited response in *Arabidopsis* is the deposition of callose, a β -1,3-glucan polymer that is believed to strengthen and plug weak or compromised sections of plant cell walls. Its deposition at the site of pathogen attack has been extensively studied. *FoCWE*, Flg22, Elf26, PGN, and OG all elicited callose deposition to varying extents and in varying patterns in wild-type Col-0 leaves, and all of these MAMPs, with the exception of Flg22, also elicited callose deposition in wild-type WS leaves. By contrast, *asFBP1.1* and the *PRX33* and *PRX34* T-DNA knockdown lines exhibited significantly reduced levels of callose deposition in response to the MAMPs (Figure 4; see Supplemental Figures 6A, 7, and 8 online). The levels of callose deposition were also quantified (see Supplemental Figure 8 online).

MAMP-elicited callose deposition has recently been shown to be dependent on the synthesis of indole glucosinolates (IGSs) (Clay et al., 2009). In turn, IGS synthesis requires the IGS biosynthetic enzymes *CYP79B2* and *CYP81F2* and the transcription factor *MYB51*. All three of the corresponding genes, *CYP79B2*, *CYP81F2*, and *MYB51*, are upregulated by MAMPs (Clay et al., 2009). The basal level of expression of these three mRNAs (Figure 5A), as well as the Flg22- or Elf26-elicited levels (Figure 5B), was significantly lower in *asFBP1.1* and the *PRX33* and *PRX34* T-DNA lines. These data are consistent with the callose deposition data shown in Figure 4 and Supplemental Figures 6A, 7, and 8 online. A fourth MAMP-elicited gene

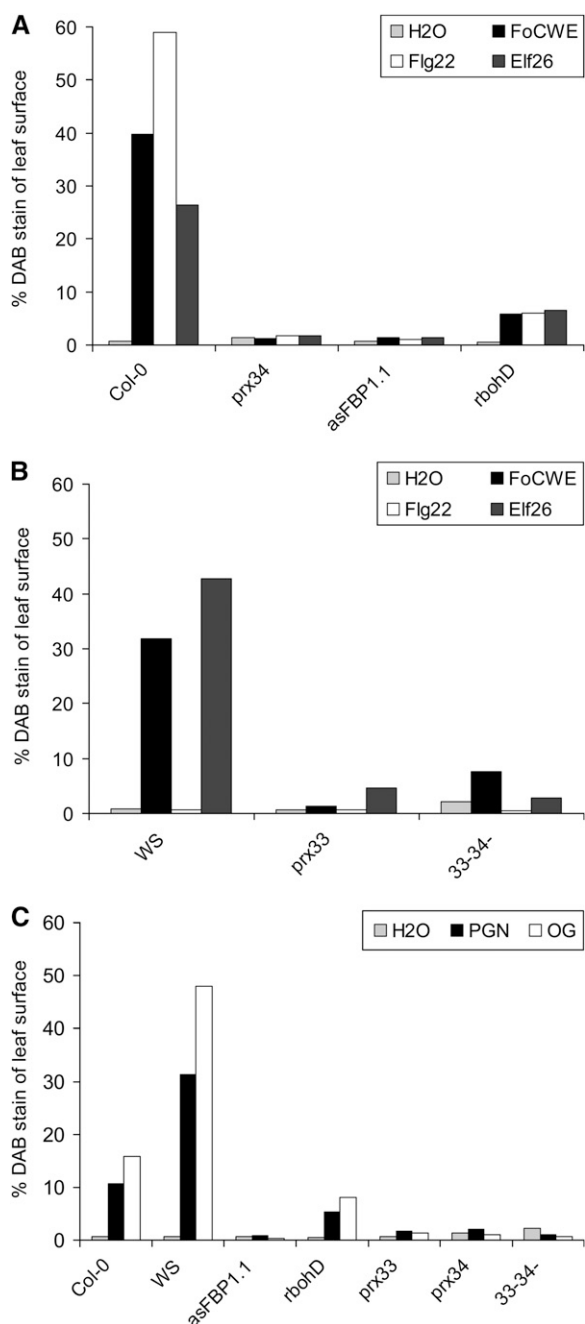


Figure 2. Hydrogen Peroxide Production Detected by DAB Staining in Mature *Arabidopsis* Leaves.

Hydrogen peroxide production detected by DAB staining was quantified as the percentage and intensity of leaf area stained. Approximately 0.1 mL of 0.5 μ M Flg22, 0.5 μ M Elf26, 100 μ g/mL FoCWE, 100 μ g/mL OG, or 100 μ g/mL PGN were infiltrated into mature rosette leaves of 23- to 25-d-old *Arabidopsis* plants. The infiltrated leaves were detached at 2 h after MAMP treatment and then stained with DAB as described in Methods. At least six independent plants were used as biological replicates, and three rosette leaves were sampled from each plant. The experiment was repeated at least two times. Representative leaves for each condition were selected for Supplemental Figures 3 to 5 online, and these leaves

(*CYP71A12*) that is involved in the biosynthesis of camalexin was also expressed at lower levels after Flg22 or Elf26 treatment (Figure 5B) in the PRX33 and PRX34 knockdown lines. Finally, as shown in Figure 1B, the transcription of the *PRX33* and *PRX34* genes themselves is activated by Flg22 or Elf26, but this activation is abrogated in the *PRX33* and *PRX34* knockdown lines. After Flg22 treatment, the level of *PRX34* mRNA was approximately 32-fold higher than *PRX33* mRNA in wild-type Col-0 plants.

Finally, we tested whether MAMP-elicited responses are completely abrogated in the *PRX33* and *PRX34* knockdown lines or whether these lines retain some residual ability to respond to MAMPs. For example, we found that whereas wild-type leaves responded to infiltration of 10 nM of Flg22 with callose deposition, no callose deposition was observed in *asFBP1.1* or *prx34:T-DNA* leaves in response to either 10 nM or 100 nM of Flg22 (see Supplemental Figure 6B online). However, after infiltration of 1 μ M of Flg22, callose deposition was observed in both of the peroxidase knockdown lines as well as in the wild type (see Supplemental Figure 6B online). These data show that *asFBP1.1* and *prx34:T-DNA* leaves can respond to Flg22, but only at Flg22 concentrations \sim 100-fold higher than those required to elicit a response in wild-type plants.

H₂O₂ Rescues the Callose Deposition–Deficient Phenotype of Peroxidase Knockdown Lines

To determine whether the abrogated responses to MAMPs in the peroxidase knockdown lines are a direct consequence of the lack of production of hydrogen peroxide, we attempted to rescue the callose deposition–deficient phenotype of the peroxidase knockdown lines after Flg22 treatment by adding exogenous H₂O₂. Indeed, H₂O₂ or Flg22 treatment in the absence of the other did not elicit any detectable callose in *asFBP1.1* or *prx34:T-DNA* leaves, but cotreatment with H₂O₂ and Flg22 together resulted in callose deposition levels similar to those observed in wild-type plants treated only with Flg22 (Figure 6). The concentrations of H₂O₂ (5 or 15 μ M) used in these experiments seem to be physiologically relevant based on the levels of H₂O₂ measured in *Arabidopsis* plant tissue challenged with *P. syringae* (M. Grant et al., 2000). These data indicate that the lack of H₂O₂ per se in the *PRX33* and *PRX34* knockdown lines results in lack of callose deposition and suggest that a lack of H₂O₂ also causes the lack of DAB staining and defense gene expression in response to MAMPs as observed in Figures 2 and 5, respectively.

were used for the quantitative analysis shown in this figure. A combination of tools from Adobe Photoshop and Cell Profiler (Carpenter et al. 2006) was used to establish the threshold of DAB staining in the leaves and distinguish the staining from the background. The final measurement used to quantify the DAB staining was the area of the stain divided by the total area of the selected representative leaf. Col-0, *prx34*, *asFBP1.1*, and *rbohD* (A); WS, *prx33* and *prx33-34-* (B); Col-0, WS, *asFBP1.1*, *rbohD*, *prx33*, *prx34*, *prx33-34-* (C) (see Supplemental Figures 3 to 5 online). *prx34*, *prx34:T-DNA*; *prx33*, *prx33:T-DNA*; *prx33-34-*, *prx33:T-DNA*; *prx34:RNAi*.

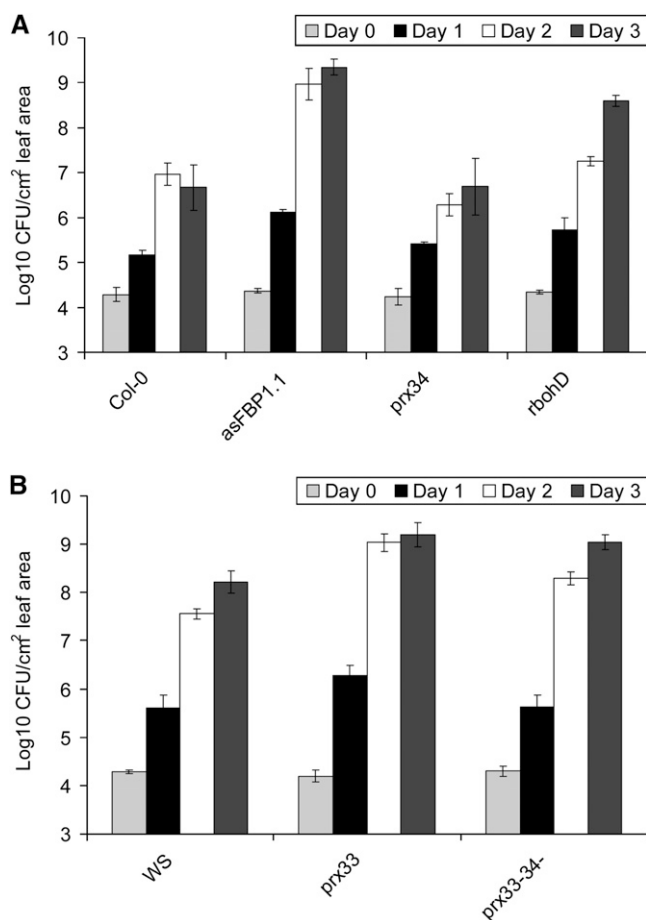


Figure 3. Growth of *P. syringae* in Mature Leaves of the Peroxidase T-DNA and Antisense Knockdown Lines.

As described in Methods, 0.1 mL of a *P. syringae* tomato strain DC3000 suspension at OD₆₀₀ = 0.0005 was infiltrated into mature rosette leaves of 23- to 25-d-old *Arabidopsis* plants, leaves were harvested at 2, 24, 48, and 72 h after infiltration, and bacterial counts were determined. Data represent the average \pm sd. Values for all four lines at 72 h after infiltration were found to be significantly different from each other except Col-0 and prx34:T-DNA with a P value < 0.05 as determined by Student's t test (A). Values for prx33:T-DNA and prx33:T-DNA;prx34:RNAi at 72 h after infiltration were found to be significantly different from WS, with a P value < 0.05 as determined by Student's t test (B). At least four biological replicates from independent plants were used for each time point, and the entire experiment was repeated with similar results. prx34, prx34:T-DNA; prx33, prx33:T-DNA; prx33-34-, prx33:T-DNA;prx34:RNAi. cfu, colony-forming units.

Comparative Roles of RBOHD and Peroxidases in MAMP-Mediated Responses

To determine the relative roles of peroxidases and NADPH oxidases in MAMP-mediated responses, we compared an *rbohD* T-DNA insertion mutant with *asFBP1.1* and the *PRX33* and *PRX34* T-DNA lines. Similar to previously reported results (Torres et al., 2002), MAMP-elicited DAB staining was absent in the *rbohD* mutant, similar to the results obtained with the peroxidase

T-DNA and antisense knockdown lines (Figure 2A; see Supplemental Figures 3 and 5 online). Unexpectedly, we found that the *rbohD* mutant was consistently modestly more susceptible to *P. syringae* pv tomato strain DC3000 than wild-type plants, although not as susceptible as *asFBP1.1* (Figure 3A). Although Chaouch et al. (2011) did not observe enhanced susceptibility of an *rbohD* mutant to *Pto* DC3000, because the *rbohD* mutant was only modestly more susceptible in our experiments, the conflicting results are probably due to differences in growth conditions. MAMP-elicited callose deposition was also modestly diminished

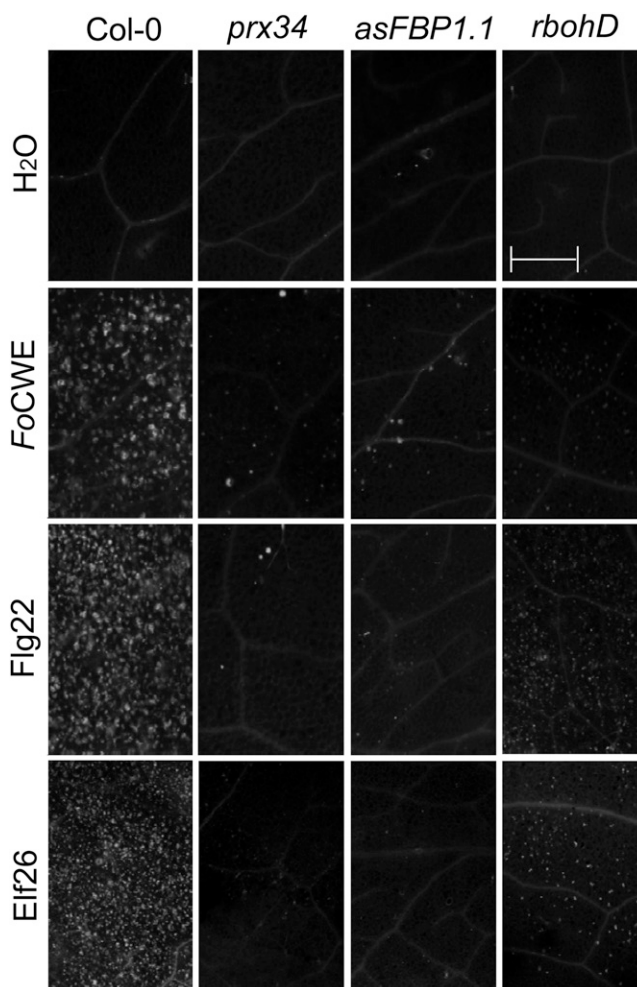


Figure 4. MAMP-Elicited Callose Accumulation Detected by Aniline Blue Staining in Mature *Arabidopsis* Leaves.

Approximately 0.1 mL of 0.5 μ M Fig22, 0.5 μ M Elf26, or 100 μ g/mL FoCWE were infiltrated into mature rosette leaves of 23- to 25-d-old *Arabidopsis* plants. At least six independent plants were used as biological replicates, and three rosette leaves were sampled from each plant. The experiment was repeated at least two times. Representative leaves are shown. Infiltrated plants were incubated at high humidity for 16 to 20 h, and then leaves were harvested and stained for callose as described in Methods. See Supplemental Figure 8 online for quantitation of the data. prx34, prx34:T-DNA.

Bar = 20 μ m.

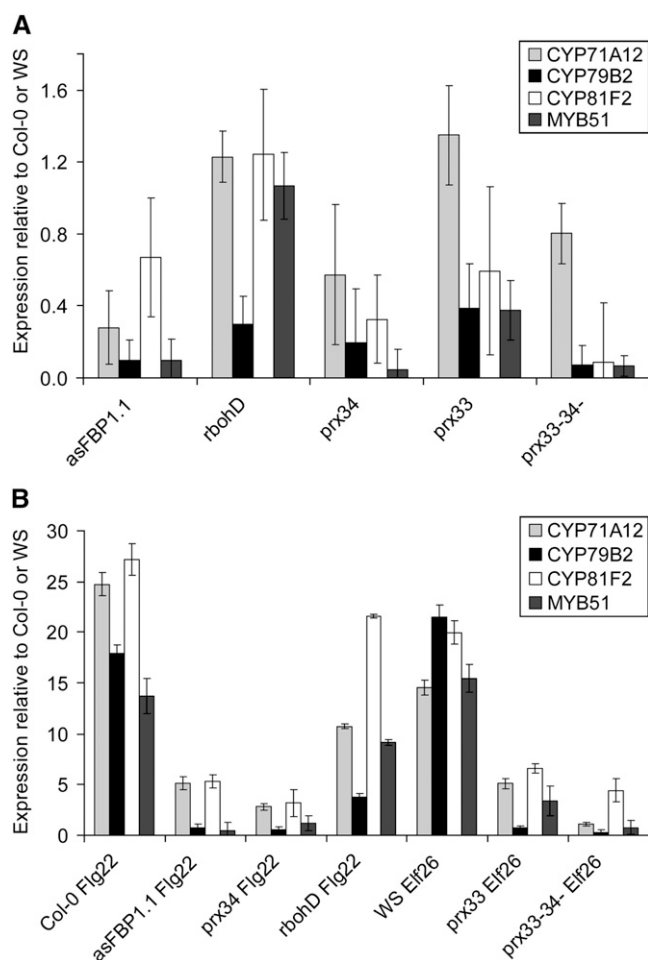


Figure 5. Quantitative RT-PCR Analysis of MAMP-Elicited Genes in Peroxidase-Downregulated Plants.

(A) Basal levels of *CYP71A12*, *CYP79B2*, *CYP81F2*, and *MYB51* mRNAs were measured in 23- to 25-d-old plants as described.

(B) Levels of *CYP71A12*, *CYP79B2*, *CYP81F2*, and *MYB51* mRNAs were measured at 2 h after infiltration of 0.1 mL of 0.5 μ M Flg22 or Eif26. Data represent the average \pm SD. All quantitative gene expression measurements were performed using technical and biological triplicates. The experiments were repeated at least two times with similar results. Values for *CYP71A12* expression in *rbohD* and *prx33* were found to be significantly different from all other expression values, with a *P* value $<$ 0.05 as determined by Student's *t* test **(A)**. Values for the gene expression levels of each of the four genes in Col-0 and WS, and all genes except *CYP79B2* in *rbohD*, were found to be significantly different from the gene expression levels of all four genes in the peroxidase knockdown lines, with a *P* value $<$ 0.05 as determined by Student's *t* test **(B)**. *prx34*, *prx34:T-DNA*; *prx33*, *prx33:T-DNA*; *prx33-34-*, *prx33:T-DNA*; *prx34:RNAi*.

in the *rbohD* mutant, especially following elicitation with the FoCWE (Figure 4; see Supplemental Figures 7 and 8 online). Finally, the *rbohD* mutant was also modestly compromised for the Flg22-mediated activation of *MYB51*, *CYP79B2*, or *CYP81F2*, which are involved in callose deposition (Figure 5B). The expression of *PRX33* and *PRX34* was not abrogated in the *rbohD* mutant before or after Flg22 treatment (Figure 1A).

DISCUSSION

In this article, we provide several lines of evidence that show that *Arabidopsis* cell wall peroxidases encoded by *PRX33* and *PRX34* play important roles in PTI elicited in response to a variety of MAMPs. A transgenic line constitutively expressing an antisense *FBP1* cDNA as well as T-DNA insertion lines targeting *PRX33* and *PRX34* exhibit a diminished oxidative burst in mature leaves after infiltration with a variety of MAMPs (Figure 2; see Supplemental Figures 3 to 5 online), including a FoCWE, synthetic peptides corresponding to flagellin (Flg22) or EF-Tu (Eif26), *Staphylococcus aureus* PGN, or pectin-derived OGs. In mature leaves of *asFBP1.1* and the *prx33/prx34* knockdown lines, the same MAMPs failed to elicit callose deposition (Figure 4; see Supplemental Figures 6A, 7, and 8 online) and failed to activate the expression of several genes previously shown to be highly induced by MAMP treatment (Figure 5). The *asFBP1.1* and *prx33* T-DNA knockdown lines (but not the *prx34:T-DNA* line) also exhibited enhanced susceptibility to the well-studied *P. syringae* pv tomato strain DC3000 (Figure 3). These data indicate a significant defect in MAMP-mediated signaling in mature *PRX33/PRX34* knockdown plants.

The observation that the *prx34:T-DNA* line did not consistently exhibit enhanced susceptibility to *P. syringae* pv tomato strain DC3000, whereas the *asFBP1.1*, *prx33:T-DNA*, and *prx33:T-DNA*; *prx34:RNAi* lines were consistently susceptible in many experiments, is in agreement with the data in Figure 1A, which shows that the T-DNA insertion in *PRX33* affected basal expression of both *PRX33* and *PRX34*, whereas *PRX33* is expressed normally in the *prx34:T-DNA* line. Indeed, it is likely that none of the *PRX33/PRX34* knockdown lines, including *asFBP1.1*, is completely deficient in peroxidase activity. Figure 1 shows that there were measurable levels of *PRX33* and *PRX34* mRNA in all of the *PRX33/PRX34* knockdown lines. Moreover, the T-DNA insertion in the *prx34:T-DNA* line is located upstream of the *PRX34* coding region. Similarly, the T-DNA insertion in *prx33:T-DNA* is in an intron, and it is likely that the mutated gene can be translated to yield at least a low level of active peroxidase. These considerations and the fact that the *Arabidopsis* genome encodes at least 73 class III peroxidases (Welinder et al., 2002; Oliva et al., 2009) make it difficult to estimate whether there is any residual activity encoded by *PRX33* and *PRX34* in the mutant lines and how much of the total peroxidase activity is accounted for by *PRX33* and *PRX34*.

The double *prx33:T-DNA*; *prx34:RNAi* knockdown line exhibited the lowest levels of *PRX33* and *PRX34* mRNA (Figure 1). This line is completely viable and does not exhibit any obvious growth or developmental defects, with the exception of larger leaves and delayed senescence. Because this double *prx33:T-DNA*; *prx34:RNAi* knockdown line does not seem to have as severe a phenotype as *asFBP1.1*, even though it has lower levels of *PRX33* and *PRX34* mRNA, it suggests that in *asFBP1.1* in addition to *PRX33* and *PRX34*, peroxidases that may have redundant functions are also knocked down.

Why Are the Peroxidase Knockdown Plants More Susceptible to Pathogens?

Because the peroxidase knockdown lines exhibit reduced ROS generation and callose deposition as well as aberrant activation

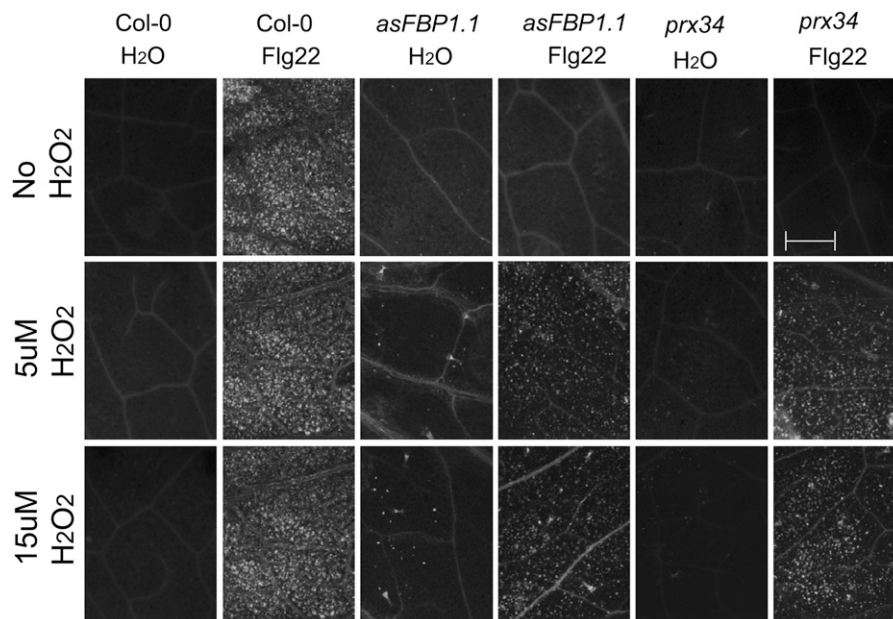


Figure 6. Exogenous H_2O_2 Application Rescues Callose Accumulation in *asFBP1.1* and *prx34*.

Approximately 0.1 mL of 0.5 μM Flg22 was infiltrated into mature rosette leaves of 23- to 25-d-old *Arabidopsis* plants. At least six independent plants were used as biological replicates, and three rosette leaves were sampled from each plant. The experiment was repeated at least two times. Representative leaves are shown. The infiltrated leaves were detached at 2 h after MAMP treatment and then placed in 12-well sterile plates overnight in 1 mL solution containing either 5 μM , 15 μM H_2O_2 , or sterile dH_2O . The leaves were then harvested and stained for callose as described in Methods. Hydrogen peroxide was applied in solution at the time of Flg22 treatment. *prx34*, *prx34:T-DNA*. Bar = 20 μM .

of MAMP-elicited transcription of defense-related genes, the simplest explanation for why these plants are more susceptible to *P. syringae* is that they are impaired in PTI. An alternative explanation, which is not mutually exclusive with a defect in PTI, is that PRX33 and PRX34 play a role in the cross-linking of cell wall or defense-related polymers. Interestingly, the peroxidase-downregulated lines exhibit larger leaves than wild-type plants, indicating that peroxidases also play a role in leaf expansion. In roots, PRX34 has been associated with cessation of elongation (Dunand et al., 2007). The role of peroxidases in this case is peroxidative cross-linking of cell wall polysaccharides, particularly pectin. By extrapolation, the leaf cell walls in the peroxidase knockdown plants may be less cross-linked. In response to pathogen challenge, a second type of peroxidative cross-linking occurs in papillae, targeted at Hyp-rich glycoproteins and Pro-rich proteins (Bradley et al., 1992; Wojtaszek et al., 1995; Brown et al., 1998). A decrease in either type of cross-linking in the peroxidase knockdown lines may contribute to enhanced susceptibility to pathogen attack.

Relative Roles of PRX33 and PRX34

It is clear from the data presented here and in Bindschedler et al. (2006) that PRX33 and PRX34 play important roles in *Arabidopsis* PTI responses, but the respective roles of PRX33 and PRX34 are not completely clear. The FBP1 antisense line *asFBP1.1* exhibits decreased levels of both basal and Flg22-elicited PRX33 and

PRX34 mRNA. Interestingly, both the *prx33:T-DNA* and *prx34:T-DNA* lines exhibit reduced levels of both PRX33 and PRX34 mRNA after Flg22-elicitation, and the basal mRNA levels of both genes are lower in the *prx33:T-DNA* line. The PRX33 and PRX34 genes (*At 3g49110* and *At 3g49120*) are adjacent in the *Arabidopsis* genome, but why the T-DNA insertion in *At 3g49120* affects expression of *At 3g49110* and vice versa under some conditions is not clear. In any case, because the expression of both peroxidase genes is affected in all the lines used in our experiments after Flg22 treatment, and because they are expressed at different levels, it is difficult to precisely sort out the relative roles of these two peroxidases.

Relative Roles of Peroxidases and NADPH Oxidases in Pattern-Triggered Immunity

Previous work (Bolwell, 1999; J.J. Grant et al., 2000; Torres et al., 2002) and the data shown here in Figure 2 and Supplemental Figures 3 to 5 online indicate that both plasma membrane-localized NADPH oxidases and cell wall peroxidases are required for a MAMP-elicited oxidative burst in mature plants. This lack of ROS in the early stages of exposure to the various MAMPs was accompanied by a lack of callose deposition after 18 h in mature leaves in the various lines with reduced levels of PRX33 and PRX34, whereas MAMP-elicited callose deposition seemed to be at least somewhat independent of the RBOHD NADPH oxidase-mediated oxidative burst (Figure 4; see Supplemental

Figures 7 and 8 online). Similarly, MAMP-elicited expression of selected defense-related genes also seemed to be more dependent on PRX33 and PRX34 than on RBOHD (Figure 5). Finally, lines in which both PRX33 and PRX34 are substantially knocked down are more susceptible to *P. syringae* than an *rbohD* mutant (Figure 3) or an *rbohF* mutant (Chaouch et al., 2011). These data suggest that the oxidative bursts generated by peroxidases and NADPH oxidases are not functionally equivalent and that peroxidases and NADPH oxidases play distinct roles in the plant defense response. ROS inhibitors tested on transgenic *Arabidopsis* cell culture lines in which the expression of PRX33 and PRX34 is downregulated by antisense expression of FBP1 cDNA show that peroxidases generate about one-half of the H₂O₂ produced in response to MAMP treatment, whereas NADPH oxidases and other sources, such as mitochondria, account for the remaining ROS production (J.A. O'Brien, unpublished data).

One important caveat with our conclusions concerning the relative roles of apoplastic peroxidases and NADPH oxidases is that our experiments only investigated the role of RBOHD in PTI, whereas previous work has suggested that RBOHD and RBOHF may have redundant roles in plant defense. An *rbohD;rbohF* double mutant, but not *rbohD* or *rbohF* single mutants, failed to exhibit an oxidative burst when infected with *P. syringae* or *H. arabidopsidis* (Torres et al., 2002). Unfortunately, under our growth conditions, the *rbohD;rbohF* double mutant exhibited a dramatic dwarf phenotype and could not be used in the experiments reported here. In addition, we attempted to cross *asFBP1.1* with *rbohD* and tested several recombinants but found that, in all cases, the expression of PRX33 and PRX34 was no longer reduced. Further experimentation will be required to fully sort out the relative roles of peroxidases and NADPH oxidases in the plant defense response.

Role of Hydrogen Peroxide in Callose Deposition

In French bean, callose accumulation is accompanied by production of H₂O₂ by the FBP1 peroxidase at sites of bacterial infection (Brown et al., 1998). Here we show in Figures 4 and 6 and Supplemental Figures 6 to 8 online that callose formation is most likely dependent on the production of hydrogen peroxide generated by a peroxidase-mediated apoplastic oxidative burst. Importantly, the lack of callose deposition in the peroxidase knockdown lines *asFBP1.1* and *prx34:T-DNA* could be rescued by the exogenous administration of physiologically relevant H₂O₂ concentrations. Consistent with the lack of callose deposition, the mRNA levels of several genes previously shown to be required for callose deposition, including the transcription factor gene *MYB51* and two cytochrome P450-encoding genes required for the synthesis of methoxylated IGSs (Clay et al., 2009; Millet et al., 2010), are downregulated in the peroxidase knockdown lines.

Peroxidase-Dependent Gene Expression and Prepriming of the Basal Defense Response

Initial ROS production, because of its rapid production, is likely performed by existing enzymes and does not require new protein synthesis. Nevertheless, there is a significant increase in the levels of PRX33 and PRX34 transcription after Flg22 elicitation,

which is not significantly affected in an *rbohD* mutant (Figure 1B). These data suggest that PRX33 and PRX34 transcription may be autoregulated by the ROS generated by PRX33 and PRX34. The basal levels of several well-studied MAMP-activated genes are also downregulated in unchallenged leaves of the *prx33* and *prx34* knockdown lines. Similar downregulation of MAMP-activated genes is also observed in transgenic *Arabidopsis* cell culture lines that are downregulated in the expression of PRX33 and PRX34 (J.A. O'Brien, unpublished data). This study also shows that several MAMP-activated proteins are depleted in CaCl₂ extracts of the PRX33/PRX34 downregulated cell culture lines. These data suggest that a low level of apoplastic ROS production may be required to preprime basal resistance. These class III peroxidases are unique, because they can generate H₂O₂ at normal physiological pH 7, whereas several other heme proteins, including catalase, require pH greater than 8 to generate H₂O₂ (Bolwell and Daudi, 2009).

Conclusions

We previously speculated that a peroxidase-generated oxidative burst may play an essential role in PTI as well as playing a role in activating NADPH oxidase during an effector-triggered HR (Bindschedler et al., 2006). The data presented in this article support this conclusion, showing that peroxidase knockdown lines are impaired in some key aspects of PTI. Overall, we have shown that the peroxidase-dependent oxidative burst generates H₂O₂, which is required for wild-type levels of several PTI-associated responses, including callose deposition and the transcriptional activation of several PTI-associated genes (*MYB51*, *CYP79B2*, *CYP81F2*) required for callose deposition. ROS generated by RBOHD is also required for some PTI responses, including an oxidative burst, but interestingly does not seem to be absolutely required for callose deposition. The latter result is consistent with the observation that the *rbohD* mutant is not compromised for Flg22-mediated activation of *MYB51*, *CYP79B2*, and *CYP81F2*. However, an important caveat is that ROS generated by either RBOHD or RBOHF may be required for callose deposition. Somewhat unexpectedly, we found that an *rbohD* mutant is more susceptible to *P. syringae* than wild-type plants, at least under the particular growth conditions used in our experiments. Because the occurrence of a peroxidase-dependent oxidative burst is a widespread mechanism that has been demonstrated in many genera, our data suggest a general role for the apoplastic peroxidase-dependent oxidative burst in the plant defense response to pathogen attack.

METHODS

Plant Material and Growth Conditions

The transgenic *Arabidopsis thaliana* line *asFBP1.1* (*H_a*) expressing a French bean (*Phaseolus vulgaris*) peroxidase in antisense orientation was described previously (Bindschedler et al., 2006). *Arabidopsis* T-DNA insertion lines in ecotypes WS and Col-0 exhibiting diminished expression of *At3g49110* (*prx33*; SALK_CS10885) or *At3g49120* (*prx34*; SALK_051769), respectively, or ecotype WS with diminished expression of both *At3g49110* and *At3g49120* (line 4.1; *prx33-34*-), were kindly provided by C. Penel at University of Geneva, Switzerland (Passardi et al., 2006). A knockdown line

altered in *At 5g47910 (rbhd)* was provided by J. Dangl at University of North Carolina at Chapel Hill (Torres et al., 2002). A T-DNA insertion line corresponding to *At 5g01075 (SALK_084805C)* was obtained from the Nottingham Arabidopsis Stock Centre. *Arabidopsis* ecotypes Col-0 or WS were used as wild-type controls and were germinated on Murashige and Skoog salts with vitamins (MS) solid media (Duchefa) after 24 h of stratification at 4°C. *Arabidopsis* transgenic seeds were germinated on MS solid media containing 50 µg/mL kanamycin. Twelve-d-old seedlings were transferred to autoclaved soil and grown in climate-controlled chambers under long day conditions (16 h light/8 h dark cycle) at 23°C.

Microbial Elicitors

The MAMPs or microbial elicitors used in this study were all prepared fresh on the day of use from stock solutions stored at -80°C. The microbial elicitors included the synthetic peptides Flg22 (Felix et al., 1999) and Elf26 (Kunze et al., 2004), which were synthesized by the Massachusetts General Hospital Peptide Synthesis and Sequencing Core Facility, Boston, Massachusetts, and used at concentrations of 0.5 µM unless otherwise indicated. A FoCWE was prepared as reported previously (Davies et al., 2006) and used at a concentration of 100 µg/mL. OGs and PGN were also used as microbial elicitors, both at concentrations of 100 µg/mL diluted in sterile deionized water. OGs were prepared as described in Ferrari et al. (2007). PGN, derived from *Staphylococcus aureus*, was acquired from Sigma-Aldrich. Diluted microbial elicitor solutions were stored on ice until required, but were brought to room temperature prior to inoculation to avoid cold stress in leaves. Leaves were also sprayed with water 30 min prior to inoculation to ease inoculum uptake and to reduce physical damage.

Dex-Inducible Constructs

Dex-inducible *FBP1* lines were generated by cloning a *FBP1* (Bindschedler et al., 2006) into pTA7001, a binary vector with a dex-inducible promoter system (McNellis et al., 1998). pTA7001 was obtained from N.-H. Chua at Rockefeller University, New York. Primers used to subclone the *FBP1* cDNA were: 5'-ACTAGTGTGTGGGGTTGTGCTT-3' (forward primer containing a *SpeI* site) and 5'-CTCGAGTAACATAGGAAACAACATCAT-GAAAA-3' (reverse primer containing a *XhoI* site). After PCR of *FBP1* cDNA using the original construct from Bindschedler et al. (2006) as the template, the resulting PCR product was cloned into pCR2.1 TOPO TA. After verifying the presence of the insert and confirming the sequence, the *FBP1* cDNA was excised and cloned into pTA7001 by digestion and ligation of the *XhoI* and *SpeI* restriction sites. pTA7001-*FBP1* DNA was transformed into *Agrobacterium tumefaciens* GV3101, and GV3101 (pTA7001-*FBP1*) was used to transform actively budding bolts of Col-0 plants as described elsewhere (Clough and Bent, 1998). F₁ transformants were selected from the resulting seed by germinating on MS media plates with 0.8% phytagar and 20 µg/mL hygromycin. F₂ progeny were collected from several F₁ hygromycin-resistant (*hyg*^r) individuals and screened for 3:1 segregation of *hyg*^r. In turn, F₃ progeny seed was collected from ~10 F₂ individuals from each line and tested for 100% *hyg*^r to identify F₂ individuals that were homozygous for the transgene cassette. A total of five dex-inducible *FBP1* lines, selected from dex-*asFBP1i.1* to dex-*asFBP1i.12*, were examined for a dex-inducible decrease in *FBP1* mRNA and for dex-inducible susceptibility to *Pseudomonas syringae* pv tomato strain DC3000.

Dex Treatments

An aqueous 10 µM solution of dex (Sigma-Aldrich) was sprayed onto mature 4-week-old plants. Control plants were sprayed with sterile dH₂O, and all plants were then kept under separate domes at high humidity for the duration of the experiment. For bacterial infections, dex was sprayed onto the plants 3 h prior to bacterial infiltration.

Mapping the *FBP1* Insertion Site in *asFBP1.1*

Mapping of the *FBP1.1* insertion site was performed by PCR-based genome walking adapting a previously described protocol (Siebert et al., 1995). Briefly, total *Arabidopsis* leaf genomic DNA (gDNA) was extracted using the cetyltrimethylammonium bromide method (Ausubel et al., 1994), and 2.5 µg of the extracted gDNA was digested overnight with *EcoRV*, *Scal*, or *HincIII*. The digested gDNA fragments were purified by phenol:chloroform and resuspended in 20 µL of dH₂O. An adaptor was designed to ligate to the gDNA fragment ends to create fragments that would serve as templates for nested PCR. The sequence of the long adaptor was 5'-GTAATACGACTCACTATAGGGCAGCGTGGTTCGACG-GCCCGGGCTGGT-3', and the sequence of the short adaptor was 5'-PO₄-ACCAGCCC-H₂N-3'. The adaptor was incubated for 2 min at 100°C and ligated to 5 µL of the digested gDNA with concentrated T4 DNA ligase (Biolabs). The reaction was incubated overnight at 16°C. After ligase inactivation, the sample was diluted 10 times in TE buffer (10 mM Tris pH 7.5, 1 mM EDTA) to a final volume of 100 µL.

Next, nested PCR was performed to amplify *FBP1*-specific fragments that would be present on the adaptor-ligated gDNA fragments after specific restriction digestion dependent on restriction sites in the *FBP1* sequence. For PCR amplification of specific sequences in the genome, four sets of primers were used: adaptor primer 1, nested adaptor primer 2, gene-specific primer 1, and gene-specific primer 2, described in Supplemental Table 1 online. The amplification of the sequence of interest was performed by two consecutive nested PCR reactions. For the first reaction, 1 µL of the diluted gDNA adapter sample was used with the adaptor primer 1/gene-specific primer 1 combination using the following thermal cycler program: seven cycles of 25 s at 95°C followed by 3 min at 72°C, then 32 cycles of 25 s at 95°C and 3 min at 67°C, and finally one cycle of 7 min at 72°C. The first PCR reaction was then diluted 1:50 and used for the nested reaction with the nested adaptor primer 2/gene-specific primer 2 combination using the following thermal cycler program: five cycles of 25 s at 95°C followed by 3 min at 72°C, then 20 cycles of 25 s at 95°C and 3 min at 67°C, and finally one cycle of 7 min at 72°C for DNA strand extension. The products of the nested PCR were analyzed using 1% agarose gel electrophoresis and then purified from the gel using the QIAquick Gel Extraction Kit (Qiagen) and sequenced (Eurofins MWG Operon).

RT-PCR and Real-Time PCR

RT-PCR was performed using a Primus 25 thermocycler (Peqlab), and qRT-PCR was performed using a Corbett Rotor-Gene (Corbett) or a Rotor-Gene Q (Qiagen). The final concentration of the RT-PCR reaction was: 0.20 µM primers, 0.2 mM deoxynucleotide triphosphate, 1.5 mM MgCl₂, and 2 µL 10 ng/µL cDNA in 5× reaction buffer together with 0.625 units of DNA Taq polymerase (GoTaq; Promega) in a total reaction volume of 50 µL. The reaction commenced at 94°C for 2 min, followed by 25 to 35 cycles of 40 s at 94°C, 40 s at 55°C, and 40 s at 70°C. The cycling reaction was completed with a final extension for 7 min at 70°C. Primer sequences used for the reactions are shown in Supplemental Table 1 online. Primers were designed using Primer 3 (www.wi.frodo.mit.edu) with gene sequences obtained from The Arabidopsis Information Resource (www.Arabidopsis.org).

For qRT-PCR, primers were designed to generate product sizes of 60 to 100 bp spanning the first intron of each target gene. Stretches of nucleotide G or C were limited to less than three where possible, and two of the last five bases on the 3' end were selected as either G or C. Primer efficiency was tested with 0.25 µM primers, 2 µL of 10 ng/µL cDNA, and 10 µL iQ SYBR-Green Supermix (Bio-Rad) or SYBR Green JumpStart Taq ReadyMix (Sigma-Aldrich) in a total reaction volume of 20 µL. The reaction commenced at 95°C for 3 min, followed by a cycling stage of 10 s at 95°C, 30 s at 55°C, and 30 s at 72°C. qRT-PCR was performed similarly

using *GAPDH*, *TUB9*, and *EIF4A* primers as the housekeeping reference genes. The PCR reaction set up was automated to reduce handling errors using a QIAgility PCR automation robot (Qiagen).

Assay for Callose Formation

In situ detection of callose was performed using aniline blue staining adapted from methods used previously (Jacobs et al., 2003; Clay et al., 2009). Briefly, three rosette leaves from 23- to 25-d-old *Arabidopsis* plants were syringe-infiltrated with ~0.1 mL of a diluted microbial elicitor solution (0.5 μ M Flg22, 0.5 μ M Eif26, 100 μ g/mL OG, 100 μ g/mL PGN, or 100 μ g/mL *FoCWE*) and placed under high humidity (~85% humidity) for 18 h. At least six independent plants were used as biological replicates, and three rosette leaves were sampled from each plant. The experiment was repeated at least two times. After infiltration and overnight incubation, leaves were harvested and placed in sterile 12-well plates. Acetic acid:ethanol (1:3) was added over 8 h with two changes to destain the chlorophyll from the leaf, followed by ethanol (50% v/v) for 1 h, ethanol (30% v/v) for 1 h, and finally dH₂O for 2 h with two changes. During the washing steps, the 12-well plates containing the leaves were placed on a constant shaker at 120 rpm to ensure even destaining and rehydration of the leaves. After that, the leaves were stained with 5 mg/mL aniline blue in 150 mM sodium phosphate (pH 7.0) for at least 30 min in the dark. Leaves were mounted in glycerol (50% v/v) and examined under fluorescence microscopy. For experiments involving exogenous H₂O₂ application, leaves were detached from the plant at 2 h after Flg22 treatment and placed in a sterile 12-well plate overnight in 1 mL of solution containing either the specified concentrations of H₂O₂ or sterile dH₂O. Callose intensity was quantified by counting the number of callose spots in images acquired from at least three leaves from each of three to six different plants (representative images shown in Figure 4 and Supplemental Figure 7 online) per line/treatment. On the y axis, a score of 10 was equivalent to saturated callose accumulation, 8 represented > 200 spots or too many to count, 5 represented ~100 spots, 3 represented ~50 spots, 2 represented five to 25 spots, and 1 represented less than five spots. The leaves included in this analysis were from at least six independent plants (three leaves each; see above).

Detection of Reactive Oxygen Species

In situ detection of hydrogen peroxide was performed by staining with DAB (Sigma-Aldrich) using an adaptation of a previous method (Thordal-Christensen et al., 1997; Bindschedler et al., 2006). Briefly, ~100 μ L of a diluted microbial elicitor solution (0.5 μ M Flg22, 0.5 μ M Eif26, 100 μ g/mL OG, 100 μ g/mL PGN, or 100 μ g/mL *FoCWE*) was infiltrated individually into mature rosette leaves from 23- to 25-d-old *Arabidopsis* plants using a needleless 1-mL syringe and infiltrated under gentle vacuum with 1 mg/mL DAB containing Tween 20 (0.05% v/v) and 10 mM sodium phosphate buffer (pH 7.0). At least six independent plants were used as biological replicates, and three rosette leaves were sampled from each plant. The experiment was repeated at least two times. Infiltrated leaves were sampled and stained after 2 h. The staining reaction was terminated 5 h after DAB infiltration, and leaves were fixed in ethanol:glycerol:acetic acid 3:1:1 (bleaching solution) placed in a water bath at 95°C for 15 min. Leaves were reimmersed in bleaching solution until chlorophyll was completely depleted and then were visualized under white light and photographed. A combination of tools from Adobe Photoshop and CellProfiler (Carpenter et al. 2006) was used to establish the threshold of DAB staining in the leaves and to distinguish the staining from the background. The final measurement used to quantify the DAB staining was the area of the stain divided by the total area of the leaf.

Inoculation and in Planta Growth Determination of *P. syringae*

P. syringae pv tomato strain DC3000 was cultured on Kings B agar (Sigma-Aldrich) containing 40 μ g/mL rifampicin. Single colonies grown for 48 h at 28°C were isolated from agar plates and transferred to Kings B or Luria-Bertani broth (Sigma-Aldrich) and grown overnight. Bacterial suspensions at OD₆₀₀ 0.2 were washed and diluted in 10 mM MgSO₄ to OD₆₀₀ 0.0005. Mature leaves of 23- to 25-d-old *Arabidopsis* plants were then infiltrated with 0.1 mL of bacterial inoculum using a needleless 1-mL syringe, and the plants were placed under high humidity (~85% humidity) for the duration of the experiment. Leaves were harvested at 24, 48, and 72 h to test for levels of bacterial growth. Control leaves were harvested 2 h after inoculation to determine the initial dose. At least four biological replicates from independent plants were used for each time point. Each biological replicate was a pooled sample of two rosette leaves from the same plant. Leaf discs of 0.5 cm diameter were homogenized using stainless steel beads (VWR) in 100 μ L of 10 mM MgSO₄ in a Qiagen TissueLyser (Qiagen) for 1.5 min at a frequency of 30/sec. Serial 10-fold dilutions were streaked on Kings B agar plates supplemented with 40 μ g/mL of rifampicin, and colonies were counted. Growth experiments shown in Figure 3 were blinded. The experimenter received the seeds of the various *Arabidopsis* lines in coded tubes from the greenhouse manager Jenifer Bush at Massachusetts General Hospital, and the code was not revealed until the in planta growth data for each line had been determined.

Statistical Analyses

Student's *t* test was performed to calculate whether the differences between distributions of data were significant using PRISM v4.0 (GraphPad Software). A *P* value of <0.05 was considered statistically significant.

Accession Numbers

Sequence data from this article can be found in the EMBL/GenBank data libraries under accession numbers *At 3g49110* (*PRX33*), *At 3g49120* (*PRX34*), *At 5g47910* (*RBOHD*), and *At 5g01075* (β -*GAL*).

Supplemental Data

The following materials are available in the online version of this article.

Supplemental Figure 1. Downregulation of *PRX33* and *PRX34*, and Growth of *P. syringae* in Mature Leaves of Dex-Inducible Peroxidase Downregulated Lines.

Supplemental Figure 2. The *asFBP1* Construct Is Inserted into a Gene with No Known Function in Disease Resistance in *asFBP1.1*.

Supplemental Figure 3. Hydrogen Peroxide Production Detected by DAB Staining in Mature *Arabidopsis* Leaves.

Supplemental Figure 4. Hydrogen Peroxide Production Detected by DAB Staining in Mature *Arabidopsis* Leaves.

Supplemental Figure 5. Hydrogen Peroxide Production Detected by DAB Staining in Mature *Arabidopsis* Leaves.

Supplemental Figure 6. MAMP-Elicited Callose Accumulation Detected by Aniline Blue Staining in Mature *Arabidopsis* Leaves.

Supplemental Figure 7. MAMP-Elicited Callose Accumulation Detected by Aniline Blue Staining in Mature *Arabidopsis* Leaves.

Supplemental Figure 8. Quantitation of Callose Intensity.

Supplemental Table 1. Quantitative Real-Time PCR and Genotyping Primers Used in This Study.

ACKNOWLEDGMENTS

We thank Annie Connery and Pauline Lim for carrying out the DAB quantitation using CellProfiler, Jenifer Bush for technical assistance, and Natalie Sykes for assistance with the DAB and callose staining. This work was supported by postdoctoral fellowships from the National Science Foundation (N.M.) and the Natural Sciences and Engineering Research Council of Canada (Z.C.), by National Institutes of Health grant R37 GM48707 and National Science Foundation grant MCB-0519898 (F.M.A.), and Biotechnology and Biological Science Research Council grant BB/E021166 (G.P.B).

AUTHOR CONTRIBUTIONS

A.D. designed the research, performed research, contributed new analytic tools, analyzed data, and wrote the article. Z.C. performed research and analyzed data. J.A.O. designed the research, performed research, and analyzed data. N.M. designed the research, performed research, and analyzed data. S.K. performed research. F.M.A. designed the research, analyzed data, and wrote the article. G.P.B. designed the research, analyzed data, and wrote the article.

Received October 24, 2011; revised December 9, 2011; accepted December 20, 2011; published January 13, 2012.

REFERENCES

- Ausubel, F.M., Brent, R., Kingston, R.E., Moore, D.D., Seidman, J.G., Smith, J.A., and Struhl, K.** (1994). *Current Protocols in Molecular Biology*. (New York: John Wiley & Sons).
- Bach, M., Schnitzler, J.P., and Seitz, H.U.** (1993). Elicitor-induced changes in Ca⁺⁺ influx, K⁺ efflux, and 4-hydroxybenzoic acid synthesis in protoplasts of *Daucus carota* L. *Plant Physiol.* **103**: 407–412.
- Bestwick, C.S., Brown, I.R., and Mansfield, J.W.** (1998). Localized changes in peroxidase activity accompany hydrogen peroxide generation during the development of a nonhost hypersensitive reaction in lettuce. *Plant Physiol.* **118**: 1067–1078.
- Bindschedler, L.V., Dewdney, J., Blee, K.A., Stone, J.M., Asai, T., Plotnikov, J., Denoux, C., Hayes, T., Gerrish, C., Davies, D.R., Ausubel, F.M., and Bolwell, G.P.** (2006). Peroxidase-dependent apoplastic oxidative burst in *Arabidopsis* required for pathogen resistance. *Plant J.* **47**: 851–863.
- Bolwell, G.P.** (1999). Role of active oxygen species and NO in plant defence responses. *Curr. Opin. Plant Biol.* **2**: 287–294.
- Bolwell, G.P., and Daudi, A.** (2009). Reactive oxygen species in plant-pathogen interactions. In *Reactive Oxygen Species in Plant Signaling, Signaling and Communication in Plants*, L.A. del Rio and A. Puppo, eds (Berlin: Springer-Verlag), pp. 113–133.
- Bolwell, G.P., Davies, D.R., Gerrish, C., Auh, C.K., and Murphy, T.M.** (1998). Comparative biochemistry of the oxidative burst produced by rose and french bean cells reveals two distinct mechanisms. *Plant Physiol.* **116**: 1379–1385.
- Bradley, D.J., Kjellbom, P., and Lamb, C.J.** (1992). Elicitor- and wound-induced oxidative cross-linking of a proline-rich plant cell wall protein: a novel, rapid defense response. *Cell* **70**: 21–30.
- Brown, I., Trethowan, J., Kerry, M., Mansfield, J., and Bolwell, G.P.** (1998). Location of components of the oxidative cross-linking of glycoproteins and of callose synthesis in papillae formed during the interaction between non-pathogenic strains of *Xanthomonas campestris* and French bean mesophyll cells. *Plant J.* **15**: 333–343.
- Carpenter, A.E., Jones, T.R., Lamprecht, M.R., Clarke, C., Kang, I.H., Friman, O., Guertin, D.A., Chang, J.H., Lindquist, R.A., Moffat, J., Golland, P., and Sabatini, D.M.** (2006). CellProfiler: Image analysis software for identifying and quantifying cell phenotypes. *Genome Biol.* **7**: R100.
- Chandra, S., Stennis, M., and Low, P.S.** (1997). Measurement of Ca²⁺ fluxes during elicitation of the oxidative burst in aequorin-transformed tobacco cells. *J. Biol. Chem.* **272**: 28274–28280.
- Chaouch, S., Queval, G., and Noctor, G.** (November 25, 2011). AtRbohF is a crucial modulator of defence-associated metabolism and a key actor in the interplay between intracellular oxidative stress and pathogenesis responses in *Arabidopsis*. *Plant J.* <http://dx.doi.org/10.1111/j.1365-3113.2011.04816.x>
- Chisholm, S.T., Coaker, G., Day, B., and Staskawicz, B.J.** (2006). Host-microbe interactions: Shaping the evolution of the plant immune response. *Cell* **124**: 803–814.
- Choi, H.W., Kim, Y.J., Lee, S.C., Hong, J.K., and Hwang, B.K.** (2007). Hydrogen peroxide generation by the pepper extracellular peroxidase CaPO2 activates local and systemic cell death and defense response to bacterial pathogens. *Plant Physiol.* **145**: 890–904.
- Clay, N.K., Adio, A.M., Denoux, C., Jander, G., and Ausubel, F.M.** (2009). Glucosinolate metabolites required for an *Arabidopsis* innate immune response. *Science* **323**: 95–101.
- Clough, S.J., and Bent, A.F.** (1998). Floral dip: A simplified method for *Agrobacterium*-mediated transformation of *Arabidopsis thaliana*. *Plant J.* **16**: 735–743.
- Davies, D.R., Bindschedler, L.V., Strickland, T.S., and Bolwell, G.P.** (2006). Production of reactive oxygen species in *Arabidopsis thaliana* cell suspension cultures in response to an elicitor from *Fusarium oxysporum*: implications for basal resistance. *J. Exp. Bot.* **57**: 1817–1827.
- Dunand, C., Crèvecoeur, M., and Penel, C.** (2007). Distribution of superoxide and hydrogen peroxide in *Arabidopsis* root and their influence on root development: possible interaction with peroxidases. *New Phytol.* **174**: 332–341.
- Felix, G., Duran, J.D., Volko, S., and Boller, T.** (1999). Plants have a sensitive perception system for the most conserved domain of bacterial flagellin. *Plant J.* **18**: 265–276.
- Fellbrich, G., Blume, B., Brunner, F., Hirt, H., Kroj, T., Ligterink, W., Romanski, A., and Nürnberger, T.** (2000). *Phytophthora parasitica* elicitor-induced reactions in cells of *Petroselinum crispum*. *Plant Cell Physiol.* **41**: 692–701.
- Ferrari, S., Galletti, R., Denoux, C., De Lorenzo, G., Ausubel, F.M., and Dewdney, J.** (2007). Resistance to *Botrytis cinerea* induced in *Arabidopsis* by elicitors is independent of salicylic acid, ethylene, or jasmonate signaling but requires PHYTOALEXIN DEFICIENT3. *Plant Physiol.* **144**: 367–379.
- Frahry, G., and Schopfer, P.** (1998). Inhibition of O₂-reducing activity of horseradish peroxidase by diphenyleneiodonium. *Phytochemistry* **48**: 223–227.
- Grant, J.J., Yun, B.-W., and Loake, G.J.** (2000). Oxidative burst and cognate redox signalling reported by luciferase imaging: Identification of a signal network that functions independently of ethylene, SA and Me-JA but is dependent on MAPKK activity. *Plant J.* **24**: 569–582.
- Grant, M., Brown, I., Adams, S., Knight, M., Ainslie, A., and Mansfield, J.** (2000). The RPM1 plant disease resistance gene facilitates a rapid and sustained increase in cytosolic calcium that is necessary for the oxidative burst and hypersensitive cell death. *Plant J.* **23**: 441–450.
- He, P., Shan, L., and Sheen, J.** (2007). Elicitation and suppression of microbe-associated molecular pattern-triggered immunity in plant-microbe interactions. *Cell. Microbiol.* **9**: 1385–1396.
- Hruz, T., Laule, O., Szabo, G., Wessendorp, F., Bleuler, S., Oertle, L., Widmayer, P., Gruissem, W., and Zimmermann, P.** (2008).

- Genevestigator v3: A reference expression database for the meta-analysis of transcriptomes. *Adv. Bioinforma.* **2008**: 420747.
- Jacobs, A.K., Lipka, V., Burton, R.A., Panstruga, R., Strizhov, N., Schulze-Lefert, P., and Fincher, G.B.** (2003). An *Arabidopsis* callose synthase, GSL5, is required for wound and papillary callose formation. *Plant Cell* **15**: 2503–2513.
- Jones, J.D.G., and Dangl, J.L.** (2006). The plant immune system. *Nature* **444**: 323–329.
- Keller, T., Damude, H.G., Werner, D., Doerner, P., Dixon, R.A., and Lamb, C.** (1998). A plant homolog of the neutrophil NADPH oxidase gp91phox subunit gene encodes a plasma membrane protein with Ca²⁺ binding motifs. *Plant Cell* **10**: 255–266.
- Kunze, G., Zipfel, C., Robatzek, S., Niehaus, K., Boller, T., and Felix, G.** (2004). The N terminus of bacterial elongation factor Tu elicits innate immunity in *Arabidopsis* plants. *Plant Cell* **16**: 3496–3507.
- Lherminier, J., Elmayan, T., Fromentin, J., Elaraqui, K.T., Vesa, S., Morel, J., Verrier, J.L., Cailleteau, B., Blein, J.P., and Simon-Plas, F.** (2009). NADPH oxidase-mediated reactive oxygen species production: Subcellular localization and reassessment of its role in plant defense. *Mol. Plant Microbe Interact.* **22**: 868–881.
- Martinez, C., Montillet, J.L., Bresson, E., Agnel, J.P., Dai, G.H., Daniel, J.F., Geiger, J.P., and Nicole, M.** (1998). Apoplastic peroxidase generates superoxide anions in cells of cotton cotyledons undergoing the hypersensitive reaction to *Xanthomonas campestris* pv. *malvacearum* race 18. *Mol. Plant Microbe Interact.* **11**: 1038–1047.
- McNellis, T.W., Mudgett, M.B., Li, K., Aoyama, T., Horvath, D., Chua, N.H., and Staskawicz, B.J.** (1998). Glucocorticoid-inducible expression of a bacterial avirulence gene in transgenic *Arabidopsis* induces hypersensitive cell death. *Plant J.* **14**: 247–257.
- Millet, Y.A., Danna, C.H., Clay, N.K., Songnuan, W., Simon, M.D., Werck-Reichhart, D., and Ausubel, F.M.** (2010). Innate immune responses activated in *Arabidopsis* roots by microbe-associated molecular patterns. *Plant Cell* **22**: 973–990.
- Oliva, M., Theiler, G., Zamocky, M., Koua, D., Margis-Pinheiro, M., Passardi, F., and Dunand, C.** (2009). PeroxiBase: A powerful tool to collect and analyse peroxidase sequences from Viridiplantae. *J. Exp. Bot.* **60**: 453–459.
- Passardi, F., Tognolli, M., De Meyer, M., Penel, C., and Dunand, C.** (2006). Two cell wall associated peroxidases from *Arabidopsis* influence root elongation. *Planta* **223**: 965–974.
- Rouet, M.A., Mathieu, Y., Barbier-Brygoo, H., and Laurière, C.** (2006). Characterization of active oxygen-producing proteins in response to hypo-osmolarity in tobacco and *Arabidopsis* cell suspensions: Identification of a cell wall peroxidase. *J. Exp. Bot.* **57**: 1323–1332.
- Siebert, P.D., Chenchik, A., Kellogg, D.E., Lukyanov, K.A., and Lukyanov, S.A.** (1995). An improved PCR method for walking in uncloned genomic DNA. *Nucleic Acids Res.* **23**: 1087–1088.
- Soylu, S., Brown, I., and Mansfield, J.W.** (2005). Cellular reactions in *Arabidopsis* following challenge by strains of *Pseudomonas syringae*: From basal resistance to compatibility. *Physiol. Mol. Plant Pathol.* **66**: 232–243.
- Thordal-Christensen, H., Zhang, Z., Wei, Y., and Collinge, D.B.** (1997). Subcellular localization of H₂O₂ in plants. H₂O₂ accumulation in papillae and hypersensitive response during the barley-powdery mildew interaction. *Plant J.* **11**: 1187–1194.
- Torres, M.A., and Dangl, J.L.** (2005). Functions of the respiratory burst oxidase in biotic interactions, abiotic stress and development. *Curr. Opin. Plant Biol.* **8**: 397–403.
- Torres, M.A., Dangl, J.L., and Jones, J.D.G.** (2002). *Arabidopsis* gp91phox homologues AtrbohD and AtrbohF are required for accumulation of reactive oxygen intermediates in the plant defense response. *Proc. Natl. Acad. Sci. USA* **99**: 517–522.
- Torres, M.A., Jones, J.D.G., and Dangl, J.L.** (2005). Pathogen-induced, NADPH oxidase-derived reactive oxygen intermediates suppress spread of cell death in *Arabidopsis thaliana*. *Nat. Genet.* **37**: 1130–1134.
- Torres, M.A., Onouchi, H., Hamada, S., Machida, C., Hammond-Kosack, K.E., and Jones, J.D.G.** (1998). Six *Arabidopsis thaliana* homologues of the human respiratory burst oxidase (gp91phox). *Plant J.* **14**: 365–370.
- Valério, L., De Meyer, M., Penel, C., and Dunand, C.** (2004). Expression analysis of the *Arabidopsis* peroxidase multigenic family. *Phytochemistry* **65**: 1331–1342.
- Welinder, K.G., Justesen, A.F., Kjaersgård, I.V.H., Jensen, R.B., Rasmussen, S.K., Jespersen, H.M., and Duroux, L.** (2002). Structural diversity and transcription of class III peroxidases from *Arabidopsis thaliana*. *Eur. J. Biochem.* **269**: 6063–6081.
- Wojtaszek, P., Trethowan, J., and Bolwell, G.P.** (1995). Specificity in the immobilisation of cell wall proteins in response to different elicitor molecules in suspension-cultured cells of French bean (*Phaseolus vulgaris* L.). *Plant Mol. Biol.* **28**: 1075–1087.